DEMS and in-situ FTIR investigations of C_3 primary alcohols on platinum electrodes in acid solutions.

Part II. Allyl alcohol

E. Pastor *, S. Wasmus and T. Iwasita

Institut für Physikalische Chemie der Universität Bonn, Wegelerstr. 12, W-5300 Bonn (Germany)

M.C. Arévalo, S. González and A.J. Arvia **

Departamento de Química Física, Universidad de La Laguna, Tenerife (Spain)

(Received 15 September 1992)

Abstract

On-line mass spectroscopy (DEMS) and in-situ Fourier transform IR spectroscopy (FTIRS) have been employed to study the electro-oxidation and the electroreduction products of allyl alcohol on Pt electrodes in acids. The electroreduction products were propanol and a mixture of propylene, propane and ethane. The main oxidation products were CO_2 and acrolein. Results are interpreted and possible mechanisms are suggested with the participation of adsorbates having different chain lengths and structures.

INTRODUCTION

The electrochemistry of compounds with ethylenic bonds is particularly interesting in relation to electrochemical hydrogenation, oxidation reactions and polymer formation. In general, hydrogenation reactions of organic compounds are highly selective. The simplest example of these reactions is the reduction of ethylene in the gas phase [1] and its electrochemical reduction in acids on different metal surfaces [2–7] yielding ethane as the main product. The latter has been identified by gas chromatography [2,3] and on-line mass spectrometry (DEMS) [5].

---

* On leave from Departamento de Química Física, Universidad de La Laguna, Tenerife, Spain.
** Visiting Professor, INIFTA, Universidad Nacional de La Plata, La Plata, Argentina.

Kinetic studies of the electroreduction of compounds with ethylenic bonds on Pt and Rh show that the reaction between the adsorbate and adsorbed H atoms formed in the preceding fast H^+ ion discharge becomes the rate-determining step [6]. The presence of substituents in the molecule influences the adsorption process itself, but does not change the electroreduction rate constant.

The kinetics of the hydrogenation of allyl alcohol (AA) adsorbed on Pt by cathodically generated H atoms has recently been studied [7]. In this study a rapid equilibrium between bulk and adsorbed AA was demonstrated. The electroreduction products from AA on Pt black electrodes in acid solution [8–10] are propane, propylene and small quantities of ethane and methane. The reductive cleavage of C–OH bonds in the allyl position with the formation of hydrocarbons has been shown for various organic compounds on platinized Pt in acids [11]. The change in the composition of the reduction products as a result of the blocking effect of previously chemisorbed species [10] has been explained by the relative contribution of different mechanisms involving the splitting of C–OH bonds and the saturation of C=C bonds, depending on the applied potential, solution composition and temperature.

Electron energy loss spectroscopy and Auger spectroscopy studies of adsorbed terminal alkenols on Pt(111) have concluded that the adsorption of AA involves the two C atoms of the C=C group and that the OH group extends away from the surface [12]. However, other studies suggest that the O atom can be also attached to the surface [13]. The adsorption and anodic stripping characteristics of AA species on polycrystalline Pt in acids [14] show that the electroadsorption of AA is potential dependent and involves the rupture of the molecule. The oxidation of AA on Pt black yields acrolein as the principal reaction product [8]. Coadsorption phenomena and multiple adsorbate interactions between AA and CO_2, CO and methanol have recently been reported [15,16]. The electro-oxidation of AA on Au [17,18] and Ru [19] in acids, has also been investigated.

The aim of the present work is to investigate the electro-oxidation and electroreduction of AA on Pt in acids employing in-situ Fourier transform IR spectroscopy (FTIRS) and DEMS. FTIRS gives information on the structure of adsorbates, whereas DEMS allows identification of products during the electrochemical reactions. The present results provide a reliable experimental basis for a mechanistic interpretation of the reactions, including the most probable intermediates participating in the process.

EXPERIMENTAL

DEMS [20,21] and in-situ FTIRS [22,23] have been employed to investigate the electrochemistry of AA on Pt in acid solutions. Runs were performed at 25°C applying the electrochemical flow cell technique using either 0.05 M H_2SO_4 or 0.1 M $HClO_4$ (Merck p.a.) as the base electrolyte and AA (Aldrich) at concentrations in the range 0.005–1 M. All solutions were prepared with Millipore Milli-Q water and deaerated with Ar or N_2. Experimental details have been given elsewhere [24].

RESULTS AND INTERPRETATION

DEMS

Electro-oxidation of bulk allyl alcohol

Cyclic voltammograms (CVs) and mass signal cyclic voltammograms (MSCVs) for AA in $HClO_4$ are shown in Fig. 1. The signal for $m/z = 57$, related to the

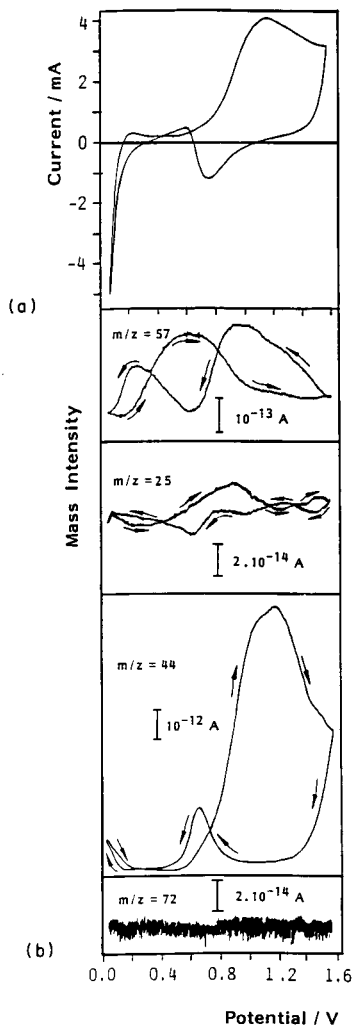Fig. 1. (a) CV in 0.01 M AA+0.1 M $HClO_4$ on porous Pt and (b) MSCVs for $m/z = 57$ (AA), $m/z = 25$ (acrolein), $m/z = 44$ (CO_2 and propane) and $m/z = 72$ (acrylic acid). (Scan rate $v = 0.01$ V s^{-1}; real area $A = 200$ cm^2).

[M-1]$^+$ fragment from AA, was used to follow the alcohol consumption. During the positive-going potential scan, this signal indicates AA consumption in two regions: below 0.20 V where reduction of AA occurs and above 0.70 V where oxidation takes place. In the reverse scan the consumption begins at 0.90 V, just as the reduction of the Pt(O) layer occurs, and decreases moderately in the potential range where AA is adsorbed until the onset of electroreduction (0.20 V) is reached again.

The signal for $m/z = 25$ was selected to show the formation of acrolein. During the positive-going potential scan, this signal begins to increase at ca. 0.40 V, reaches a maximum at 0.80 V and then remains relatively constant in the Pt(O) region.

The signal for $m/z = 44$ indicates that the threshold potential for the production of CO_2 in the positive-going potential scan is 0.50 V. This signal displays a broad peak at ca. 1.10 V which can be attributed to different reactions producing CO_2. Moreover, a reactivation signal at 0.65 V can be seen during the reverse scan. In the 0.05–0.20 V range, the $m/z = 44$ signal reveals the formation of propane.

No potential-dependent $m/z = 72$ signal ([acrylic acid]$^{\cdot +}$) was observed, and so we conclude that no acrylic acid from the oxidation of AA can be detected by DEMS.

Electroreduction of bulk allyl alcohol

Several electroreduction products were detected in the Pt(H) region below 0.25 V (Fig. 2). The most representative m/z values are 59 ([M − 1]$^+$ fragment from propanol), 44 from [propane]$^{\cdot +}$ (see Fig. 1), 38 ([C_3H_2]$^+$ fragment from propylene) and 30 from [ethane]$^{\cdot +}$ (see Fig. 1). The signals for $m/z = 30$ and $m/z = 38$ include small contributions from propane and propanol.

After taking into account the fragmentation values and the superimposed contributions of fragments from different molecules (Table 1 [25]), the following yields were determined: 76% propane, 17% propylene and 7% ethane. Except for ethane, there is a good agreement with literature results obtained by gas chromatography analysis of the products during potential-controlled electrolysis [9]. At 0.08 V, 79% propane, 20% propylene and 0.9% ethane were found. The differences may be due to the different experimental conditions. The production of propanol, which was not considered in the percentage yields given above, is about half that of ethane.

Electro-oxidation of allyl alcohol adsorbate

After adsorption a flow cell procedure was used to replace the electrolyte by pure base solution. The adsorbed residues remaining on the electrode surface were then analyzed during a subsequent potential scan. The results are given in Fig. 3(a). The only product resulting from the electro-oxidation of AA adsorbates formed at different potentials is CO_2. The shape of the signal for $m/z = 44$ reveals that at least two different processes occur during anodic stripping, one with a maximum at ca. 0.90 V (E_{p_1}) and a second one (E_{p_2}) in the Pt(O) region.

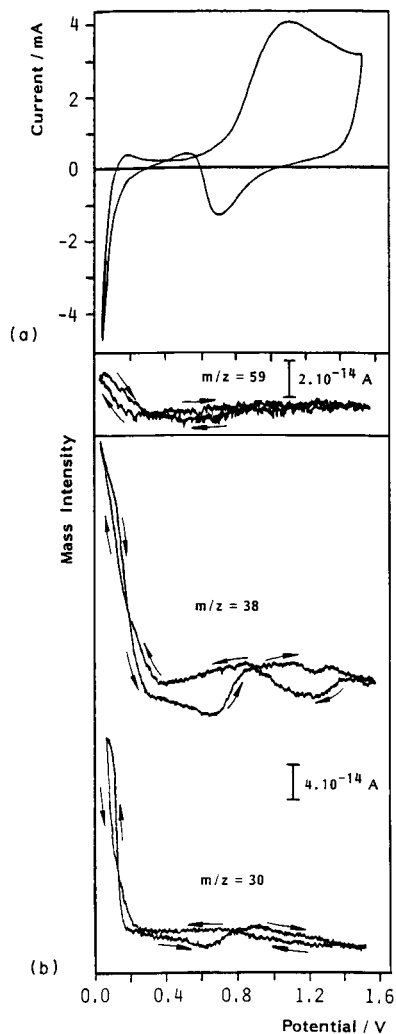Fig. 2. (a) CV in 0.01 M AA + 0.1 M HClO$_4$ on porous Pt and (b) MSCVs for $m/z = 59$ (propanol), $m/z = 38$ (propylene) and $m/z = 30$ (ethane). Only the Pt–H potential region is shown. (Scan rate $v = 0.01$ V s^{-1}; real area $A = 200$ cm^2).

The adsorbed residues cannot be completely oxidized in one cycle even if the potential is held for 15 min at 1.55 V. At least two cycles at 0.01 V s^{-1} are required to complete the oxidation (Fig. 3(b)). These remaining residues are responsible for the third CO$_2$ peak (E_{p_3}) observed in the negative potential scan during the electrodesorption of Pt(O).

Peak potentials and charges depend on the adsorption potential. Table 2 lists the peak potentials taken from the MSCVs and the oxidation charges under the

TABLE 1

Relative intensity of mass spectrometry signals of fragments related to possible compounds of interest for the present work

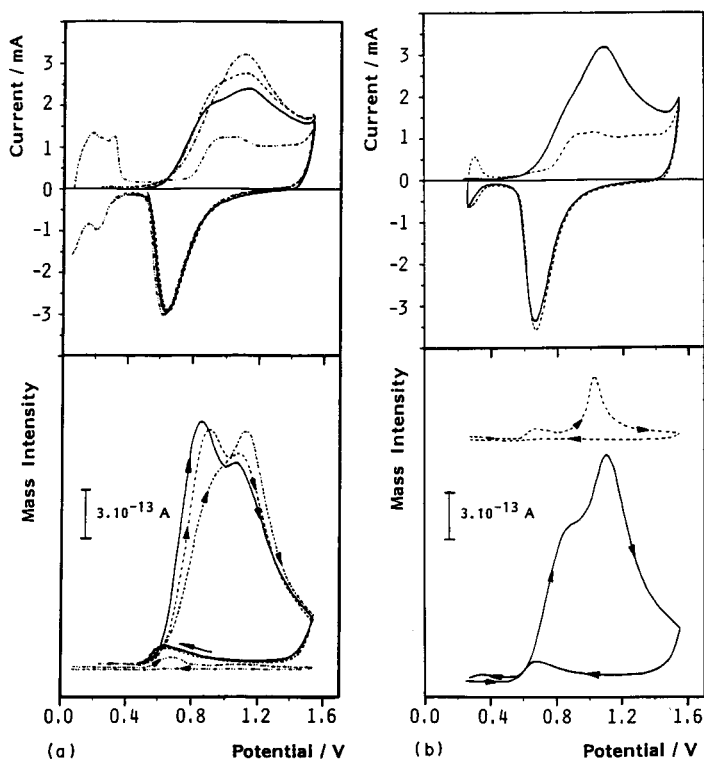| Compound	m/z									
	15	25	26	30	38	44	57	59	72	Total
Methane	815	–	–	–	–	–	–	–	–	1977
Ethane	33	30	211	269	–	–	–	–	–	2143
Propane	42	4	70	18	49	336	–	–	–	3267
Propylene	27	14	83	–	174	1	–	–	–	3528
n-Propanol	12	4	32	21	18	7	4	113	–	2002
AA	32	31	137	186	70	1	1000	11	–	4149
Acrolein	5	90	588	11	7	2	24	–	–	3957
Acrylic acid	5	95	351	2	4	113	4	2	1000	3968

From ref. 25.

Fig. 3. (a) CVs during the electro-oxidation of AA adsorbates in 0.1 M $HClO_4$ and MSCVs for $m/z = 44$ (CO_2) ($v = 0.01$ V s^{-1}; $A = 175$ cm^2). (a), —— $E_{ad} = 0.55$ V; ------ $E_{ad} = 0.40$ V; –·–·– $E_{ad} = 0.22$ V; –··– $E_{ad} = 0.05$ V. (b), $E_{ad} = 0.22$ V; —— first cycle; – – – second cycle.

TABLE 2

Potentials E_{p_1}, E_{p_2} and E_{p_3}, of the voltammetric anodic peaks ($v = 0.01$ V s^{-1}) related to the first electro-oxidation cycle of AA adsorbates formed on Pt at E_{ad}

Base electrolyte	E_{ad} /V	N_H	E_{p_1} /V	E_{p_2} /V	E_{p_3} /V	q_{ox} /mC
0.05 M H$_2$SO$_4$	0.40	4	0.74	1.08	0.68	54
	0.22	4	0.69	1.07	0.65	43
	0.50	0	0.89	1.09	0.67	86
	0.40	0	0.93	1.12	0.67	102
	0.22	0	0.95	1.14	0.65	106
0.1 M HClO$_4$	0.40	4	0.67	1.07	0.75	58
	0.22	4	0.65	1.07	0.69	44
	0.40	0	0.87	1.10	0.69	100
	0.22	0	0.87	1.12	0.69	99

N_H, number of cycles in the Pt–H potential region; q_{ox}, electro-oxidation charge of AA adsorbates; area of working electrode, 175 cm^2.

first and second peaks taken from the CV experiments. As the potential is made more negative in the potential range 0.20–0.50 V, the oxidation charge grows. At the same time, a predominance of the processes under the second peak is observed, i.e. the distribution of species on the electrode surface is affected by the adsorption potential. Obviously, adsorbates with a higher degree of oxidation (oxygen-containing species) are responsible for the first peak.

The base electrolyte has a pronounced influence on the peak potentials. All processes seem to be hindered more in H$_2$SO$_4$ than in HClO$_4$, as we can conclude from the positive shifts of E_{p_1} and E_{p_2} and the negative shift of E_{p_3} in H$_2$SO$_4$. This effect was also observed during the oxidation of strongly adsorbed species from n-propanol [24]. HSO$_4^-$ ions adsorbed on Pt [26] seem to exert long-range effects through the formation of hydrogen bonds with water [27]. The adsorbed residues, in particular those containing oxygen, may be involved in the resulting structure, and thus its oxidation will be more difficult.

Electroreduction of allyl alcohol adsorbate

During potential scans in the hydrogen region, AA adsorbates are reduced to hydrocarbons. Production of propane, propylene and ethane is shown in Fig. 4. The largest amount of propane, propylene and ethane is produced during the first cycle and production drops to zero on the fourth cycle. Hydrogenation via adsorbed species has been reported in the literature [6–11] but has not been demonstrated directly. The propane : propylene : ethane yield ratio, calculated from the respective mass intensities of the three hydrocarbons during the first cycle, is 1 : 1 : 1. This result indicates the cleavage of the C$_3$ chain in one out of three adsorbed AA molecules yielding a C$_2$ hydrocarbon and an oxygen-containing residue. The presence of several adsorbates can be linked to the peak multiplicity observed in the MSCVs for $m/z = 44$ at high potentials during the direct anodic stripping of AA adsorbates (Fig. 3).
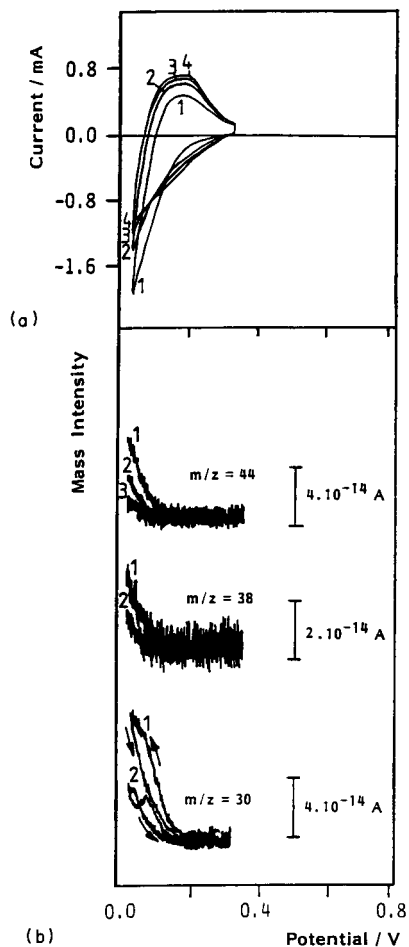
Fig. 4. (a) CVs corresponding to the electroreduction of AA adsorbates to hydrocarbons; (b) MSCVs for $m/z = 30$ (ethane), $m/z = 44$ (propane) and $m/z = 38$ (propylene) during continuous cycling between $E_{ad} = 0.40$ V and $E = 0.05$ V ($v = 0.01$ V s^{-1}; 0.05 M H$_2$SO$_4$; $A = 175$ cm^2). The numbers indicate successive potential sweeps.

The relative yields for hydrocarbon formation from AA adsorbates differ to some extent from those obtained during the electroreduction of bulk AA. This difference may be caused by the different experimental procedure. While the reduction of the adsorbate was measured after adsorbing AA at a definite potential during 10 min, the bulk results were obtained during stationary repetitive potential scans. Thus, in the potentiodynamic experiment, the adsorption kinetics can affect the relative product yields.

The electro-oxidation of residual AA adsorbates remaining after cycling the potential in the H adatom potential region (Fig. 5) generates a new current peak in
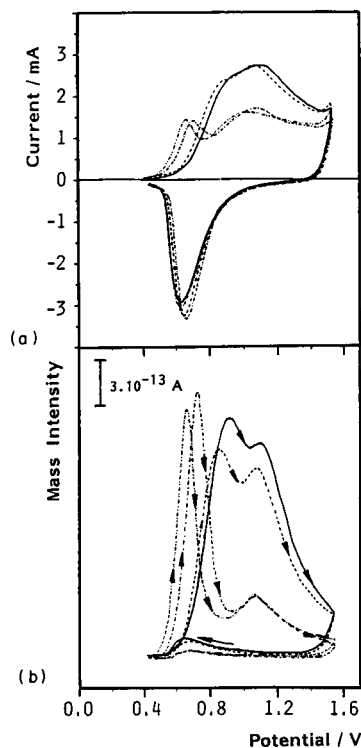
Fig. 5. (a) CVs corresponding to electro-oxidation of AA adsorbates and (b) MSCVs for $m/z = 44$ (CO_2) ($E_{ad} = 0.40$ V; $v = 0.01$ V s^{-1}; $A = 175$ cm^2): ———— direct oxidation of the adsorbate in 0.05 M H_2SO_4; – · – · – oxidation after four cycles in the Pt–H potential region; - - - - - - direct oxidation of the adsorbate in 0.1 M $HClO_4$; – · · – oxidation after four cycles in the Pt–H potential region.

the CV and a corresponding CO_2 signal in the MSCV at ca. 0.65 V in $HClO_4$. Again, there is a positive shift (ca. 0.70 V) in H_2SO_4. Since this is the electro-oxidation potential range of CO adsorbates on Pt [16,20], it is likely that during the electroreduction of O-containing adsorbates a cleavage of the C_3 chain occurs, producing a C_2 hydrocarbon and an adsorbed CO fragment.

The electro-oxidation charge of the residual adsorbates after four reduction cycles falls to about 50%–60% of the original value for $E_{ad} = 0.22$ V, and to ca. 40%–45% for $E_{ad} = 0.40$ V (Table 2). In addition, CVs and MSCVs for $m/z = 44$ also show a weaker contribution at ca. 1.10 V. The intensity of this signal appears to be independent of the solution composition. A very weak contribution of the CO_2 signal can also be seen during the first negative-going potential scan. In general, these results resemble those previously described for n-PrOH adsorbates [24].

In-situ FTIRS

As we have shown in the preceding sections, either electro-oxidation or electroreduction of AA can occur depending on the applied potential. Moreover, the nature of the adsorbed species is also potential dependent. This critical point has to be taken into account in the experimental procedure used to obtain the IR spectra. In all cases, after activation of the electrode in the base electrolyte (0.5 M $HClO_4$) the potential was held at 0.25 V or 0.40 V and the alcohol-containing solution was introduced into the cell. Spectra were taken (i) with AA present in the bulk of the solution or (ii) with the adsorbate after exchange of the electrolyte with pure base solution.

Bulk experiments

After recording a reference spectrum at 0.25 V, the potential was stepped to more positive values where the sample spectra were recorded. Figure 6 shows spectra for AA at different concentrations in the range 10^{-2}–1 M. The fact that no bands related to bulk AA consumption could be observed may be the result of both the prevalence of surface processes and the weak characteristics of the AA bands themselves [28]. The bands at 1640 cm^{-1} and 1120 cm^{-1} correspond to H_2O and ClO_4^- ions respectively.

The CO_2 production is rather insensitive to the AA concentration. Figure 6(a) shows that the strong band at 2341 cm^{-1}, which is due to the asymmetric stretching of CO_2, increases by a factor of 1.5 when the concentration is changed by a factor of 100. This indicates that the CO_2 production is mainly related to electro-oxidation of AA adsorbate rather than bulk AA. Also, the weak positive band at 2015 cm^{-1} (Fig. 6(b)), which can be assigned to the C–O stretching frequency of linearly adsorbed CO, is almost independent of the bulk AA concentration.

A strong band with a maximum at 1687 cm^{-1} (carbonyl group), a very weak band at 1430 cm^{-1} and a weak band at 1365 cm^{-1} (Figs. 6(c) and 6(d)) are very sensitive to the AA concentration. These bands are related to the electro-oxidation of bulk AA and can undoubtedly be assigned to acrolein as a solution product, as confirmed by spectra taken with s polarized light. No acrylic acid was observed. *

FTIR spectra of adsorbed species

The methodology described here allowed us to obtain *absolute* bands for adsorbed species. This procedure must be employed to detect adsorbates presenting bands with frequencies which are rather insensitive to the applied potential.

The adsorbate spectra were obtained at $E_{ad} = 0.40$ V and $E_{ad} = 0.25$ V. In both cases, after adsorption from 0.005 M AA solution and electrolyte replacement by

---

* If acrylic acid were present, the carbonyl band would be accompanied by other characteristic bands at 1240 and 1300 cm^{-1}.
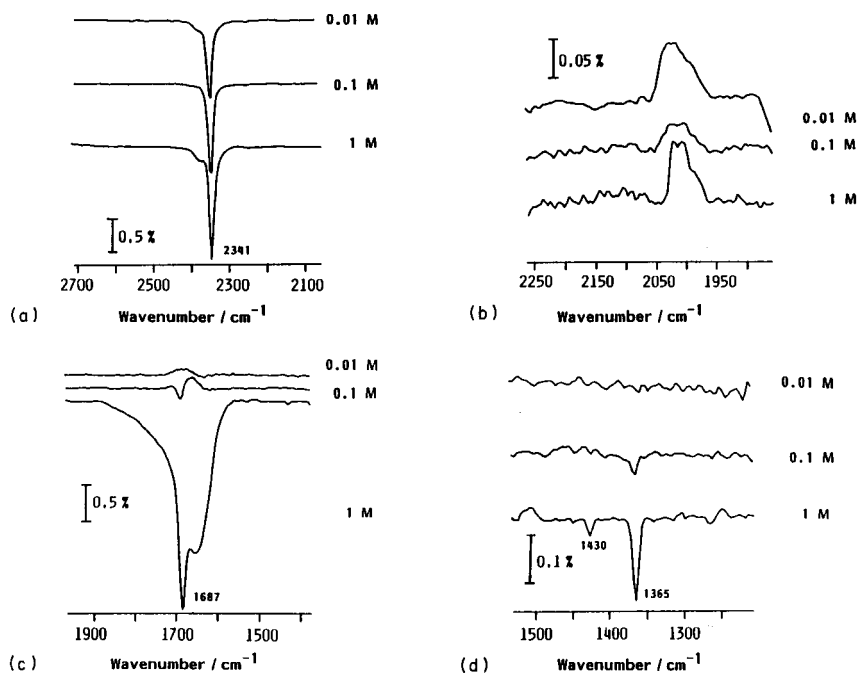
Fig. 6. Comparison of FTIR spectra (256 scans each, 8 cm^{-1}) obtained for 0.01 M, 0.1 M and 1 M AA in 0.5 M HClO$_4$ on polycrystalline Pt at 0.90 V: (a), (b), (c) and (d) correspond to different parts of the spectra. The reference spectrum was taken at 0.250 V.

0.5 M HClO$_4$, a reference spectrum R_0 was recorded at E_{ad}. A potential step to 1.50 V was then applied in order to oxidize most of adsorbed residues. Finally, the potential was reset to E_{ad} and a sample spectrum R was obtained at this potential. In this way, the spectra, calculated as R/R_0, present positive-going bands for the adsorbates oxidized at 1.50 V.

The reflectance spectra in Fig. 7 were obtained at $E_{ad} = 0.40$ V (Fig. 7(a)) and $E_{ad} = 0.25$ V (Fig. 7(b)). The bands at 2960 cm^{-1}, 2920 cm^{-1} and 2850 cm^{-1} can be related to CH$_3$ asymmetric stretching, CH$_2$ asymmetric stretching and CH$_2$ symmetric stretching respectively. The CH$_3$ symmetric stretching band appears as a shoulder at ca. 2870 cm^{-1} [29–31]. The relative intensities of these bands depend on E_{ad}. Since AA contains no CH$_3$ groups, it is clear that hydrogenation of the molecule occurs during the adsorption. Moreover, the intensities of the features at 2960 cm^{-1} and 2920 cm^{-1} reflect the concentrations of CH$_3$ and CH$_2$ respectively. For $E_{ad} = 0.40$ V the intensity of the CH$_2$ asymmetric stretch is twice the intensity of the CH$_3$ asymmetric stretch, whereas for $E_{ad} = 0.25$ V the two bands have almost equal intensities. Therefore we conclude that at 0.25 V the CH$_3$ content increases at the expense of CH$_2$.

The negative-going band at 2343 cm^{-1} is due to CO$_2$ produced during the oxidation step at 1.50 V. The feature at 2040 cm^{-1} is due to the C–O stretching of
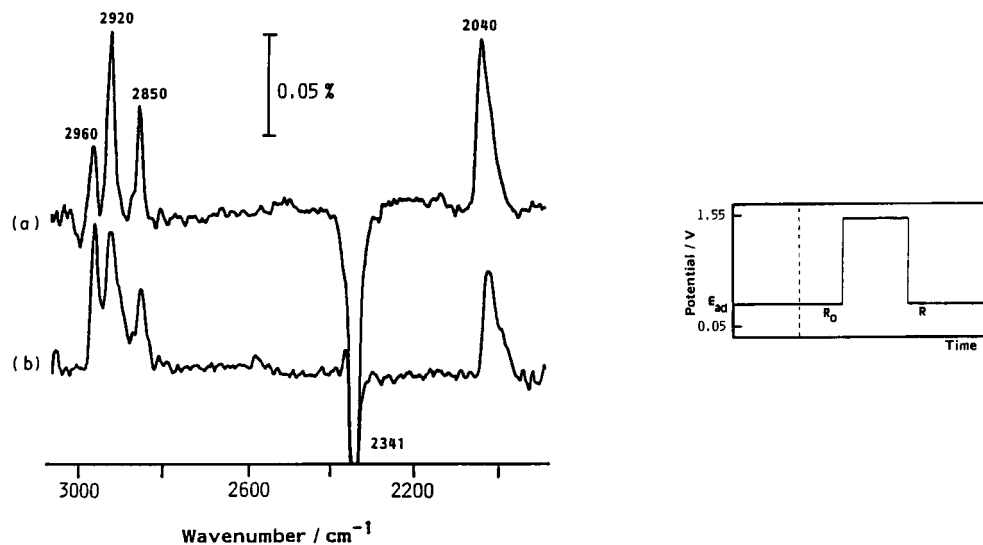
Fig. 7. Reflectance spectra (1000 scans each, 8 cm^{-1} resolution) corresponding to the electro-oxidation of AA adsorbates on polycrystalline Pt: (a) $E_{ad} = 0.40$ V; (b) $E_{ad} = 0.25$ V. The potential program is shown in the insert. Electrolyte replacement is indicated by the broken line.
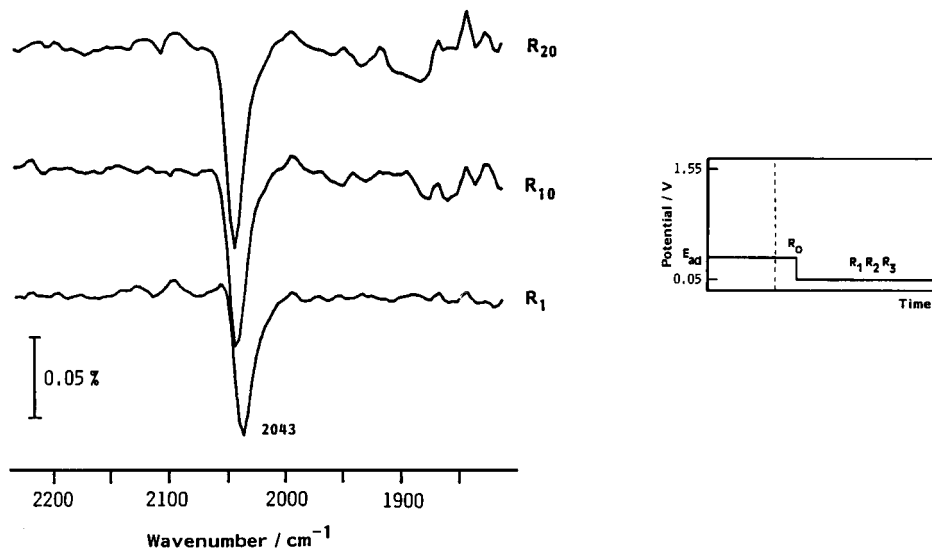

Fig. 8. Reflectance spectra (1000 scans each, 8 cm^{-1} resolution) at 0.05 V taken at different times showing CO formation during the electroreduction of AA adsorbates. R_1 corresponds to ca. 5 min, R_{10} corresponds to ca. 50 min and R_{20} corresponds to ca. 100 min. The reference spectrum was obtained at $E_{ad} = 0.40$ V. The potential program is shown in the insert. Electrolyte replacement is indicated by the broken line.

linearly adsorbed CO. Additional bands related to C–H stretching from groups like C=CH$_2$ or H–C=C–H might be expected from AA adsorbates. However, the detection of these bands is extremely difficult because they are very weak [1] and they should be located at frequencies greater than 3000 cm^{-1} which overlap the OH stretch of H$_2$O.

In a second experimental approach, the potential was set to 0.05 V after recording a reference spectrum at E_{ad}, the adsorbates were electroreduced and
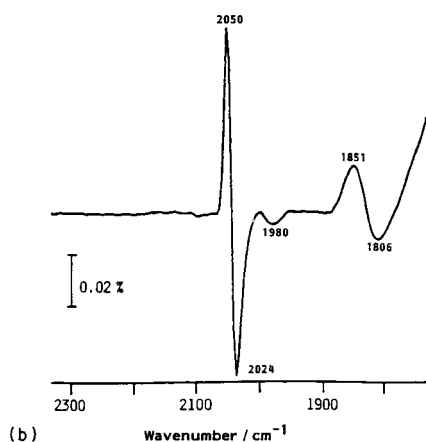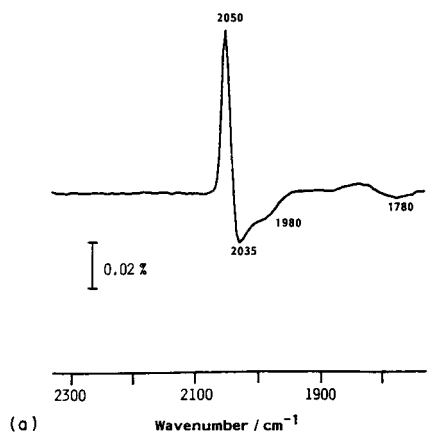

Fig. 9. FTIR reflectance spectra taken by means of alternating potential steps. The reference potential was 0.40 V and the sample potentials were (a) 0.22 V and (b) 0 V. Thirty thousand interferograms were collected at each potential. The potential was changed every 1000 scans.

successive reflectance spectra were recorded. The resulting spectra show the production of linearly bonded CO (gain band at 2043 cm^{-1} (Fig. 8)) which slowly increases with the electroreduction time as shown by the band intensities: $(8.1 \times 10^{-2})\%$ for the first spectrum (5 min), $(10.2 \times 10^{-2})\%$ for the tenth spectrum (ca. 50 min) and $(11.6 \times 10^{-2})\%$ for the twentieth spectrum (ca. 100 min).

Finally, spectra for adsorbed AA were obtained by applying a potential modulation between 0.40 V (reference potential) and either 0.22 V (Fig. 9(a)) or 0 V (Fig. 9(b)). No bands were observed in the 2800–3000 cm^{-1} region. The strong bipolar band at 2050–2035 cm^{-1} is due to linearly bonded CO, the weak band at 1980 cm^{-1} is assigned to double-coordinated CO and the medium band at 1851–1806 cm^{-1} corresponds to triple-bonded CO [32–34]. These spectra resemble those already obtained for n-PrOH adsorbed residues on Pt using a similar procedure [24].

DISCUSSION

Summary of the experimental results

In order to establish the nature of the adsorbed intermediates we can summarize the experimental results accompanying the electroadsorption of allyl alcohol on platinum as follows.
(i) During the adsorption of AA on Pt, anodic or cathodic current transients were observed, depending on the applied potential [14].
(ii) DEMS results show that the electroreduction of bulk AA, which occurs in the Pt(H) region (ca. 0–0.25 V), yields propane, propylene, ethane and propanol. The cleavage of the C_3 chain to form ethane occurs to a very small extent during the electroreduction of bulk AA under potentiodynamic conditions (propane:propylene:ethane ratio of 0.76:0.17:0.07).
(iii) According to DEMS, the electroreduction of strongly adsorbed intermediates yields hydrocarbons in the propane:propylene:ethane ratio of 1:1:1.
(iv) FTIRS shows the presence of CH$_3$- and CH$_2$-containing species. The CH$_3$:CH$_2$ ratio increases as the adsorption potential is made more negative. FTIR spectra demonstrate that the amount of linearly adsorbed CO slowly increases during the reduction at 0.05 V.
(v) As demonstrated by DEMS and FTIRS, the electro-oxidation of bulk AA produces the unsaturated aldehyde (acrolein) and CO$_2$, while electro-oxidation of the adsorbate produces only CO$_2$.
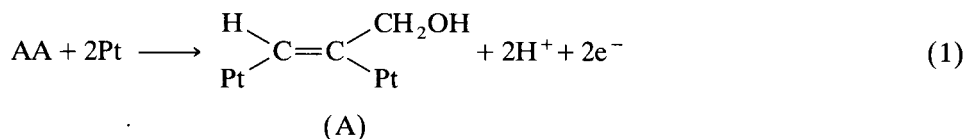Further considerations involve the chemical properties of allyl compounds.
(vi) Three different metal + AA interactions can be considered: Pt + vinyl H atoms, the Pt + π-electron system from AA and the Pt + CH$_2$OH group interactions [35].
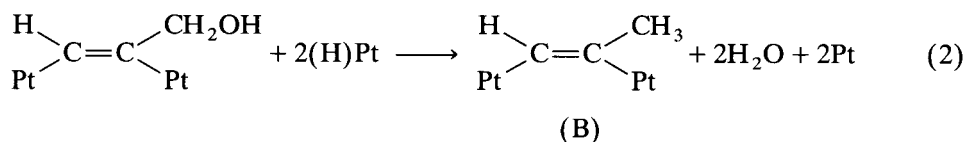
Possible adsorbate structures

The results summarized in the previous section allow us to suggest that the electrochemical behavior of AA on Pt in acid solutions is similar to that of

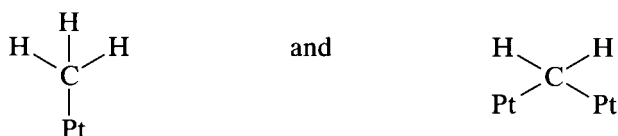ethylene on Pt [36]. Accordingly, the adsorption occurs with abstraction of vinyl hydrogen atoms as follows:

$$\text{AA} + 2\text{Pt} \longrightarrow \underset{\text{Pt}}{\overset{\text{H}}{\diagup}}\text{C}{=}\text{C}\underset{\text{Pt}}{\overset{\text{CH}_2\text{OH}}{\diagdown}} + 2\text{H}^+ + 2\text{e}^- \tag{1}$$

$$(\text{A})$$

In this reaction the CH_2OH group from AA remains intact in adsorbate A, and this explains the appearance of CH_2 group bands in the spectrum. The formation of CH_3 groups becomes possible through the interaction with Pt(H) in a reaction predominating at low potentials:

$$\underset{\text{Pt}}{\overset{\text{H}}{\diagup}}\text{C}{=}\text{C}\underset{\text{Pt}}{\overset{\text{CH}_2\text{OH}}{\diagdown}} + 2(\text{H})\text{Pt} \longrightarrow \underset{\text{Pt}}{\overset{\text{H}}{\diagup}}\text{C}{=}\text{C}\underset{\text{Pt}}{\overset{\text{CH}_3}{\diagdown}} + 2\text{H}_2\text{O} + 2\text{Pt} \tag{2}$$

$$(\text{B})$$

It must be considered that hydrogenation of allyl hydroxyl groups on Pt or Pd as catalysts readily produces hydrogenolysis, i.e. rupture of the C–O bond [37].
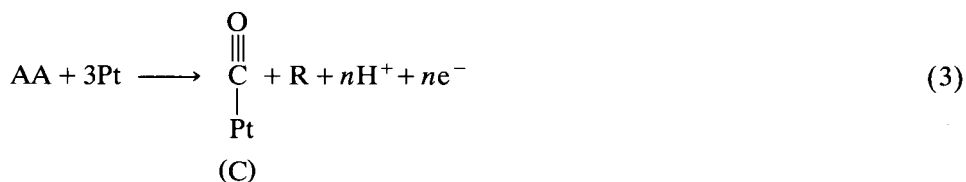
According to the surface selection rule [22], no IR activity is expected for the double bond between two carbon atoms attached to the surface. However, the positions of the CH_2 and CH_3 groups in species A and B allow the dipole moment component of both the symmetric and asymmetric modes to interact with the electric field of p-polarized radiation, in agreement with the surface selection rule.

For adsorbed species such as

$$\text{H}\diagdown\underset{\underset{\text{Pt}}{|}}{\overset{\overset{\text{H}}{|}}{\text{C}}}\diagup\text{H} \qquad \text{and} \qquad \text{H}\diagdown\underset{\text{Pt}\diagup\diagdown\text{Pt}}{\text{C}}\diagup\text{H}$$

only the symmetric modes should be active for p-polarized light. In addition, further hydrogenation would produce methane; this product was not detected in the DEMS experiments. Therefore we can rule out $CH_3(Pt)$ or $CH_2(Pt)$ as adsorbates.

FTIRS experiments demonstrate the formation of linearly bonded CO during the adsorption process. The presence of this species can be understood through the rupture of the AA molecule, simultaneously yielding a residual adsorbate R with two C atoms, the nature of which cannot be easily established:

$$\text{AA} + 3\text{Pt} \longrightarrow \underset{\underset{\text{Pt}}{|}}{\overset{\overset{\text{O}}{|||}}{\text{C}}} + \text{R} + n\text{H}^+ + n\text{e}^- \tag{3}$$

$$(\text{C})$$

Species containing the oxygen atom in the chain should also be formed. These species are responsible for the small increase in the quantity of adsorbed CO as the potential is set below 0.25 V. Such a structure must involve the attack of the methylene group and the bonding of the α-C atom to a single Pt site. Tentatively we suggest that the carbon chain is set perpendicular to the surface:

$$AA + Pt \longrightarrow CH_2 = CH - \overset{\overset{\displaystyle O}{\|}}{C} - Pt + 3H^+ + 3e^- \tag{4}$$

$$(D)$$
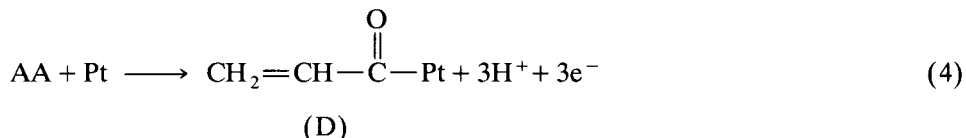
This species needs free places on the Pt surface to be oxidized and may be responsible for the oxidation peaks during the second voltammetric cycle (Fig. 3(b)). If adsorbate D is present in a low concentration, its identification via the IR spectrum may be very difficult.
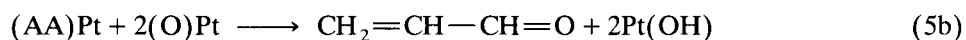
Finally, on a positively charged Pt electrode (pzc = 0.19 V [38]) the overlapping of π orbitals from AA with empty Pt d orbitals could lead to a planar structure AA (Pt) with the two groups of sp^2 orbitals lying planar to the platinum surface. In this case no molecular bonds are broken and a weaker interaction should be expected, in contrast with adsorbates A–D. Such adsorbed molecules are in equilibrium with the bulk species and can be desorbed during electrolyte exchange.

Oxidation reactions

In the presence of bulk AA weakly adsorbed molecules forming a planar structure as described above can interact with (OH)Pt or (O)Pt to form acrolein:

$$(AA)Pt + 2(OH)Pt \longrightarrow CH_2 = CH - CH = O + 2H_2O + 2Pt \tag{5a}$$
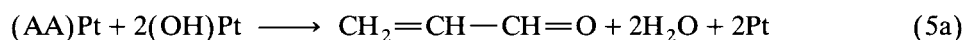
or, at potentials above 1.0 V,

$$(AA)Pt + 2(O)Pt \longrightarrow CH_2 = CH - CH = O + 2Pt(OH) \tag{5b}$$

As a support for the participation of weakly adsorbed AA in reactions (5a) and (5b), we should consider that AA is able to act as a donor of π electrons in complexes with transition metals. In such complexes the methylene group, to which the –OH group is attached, can be preferentially attacked by oxidant agents yielding acrolein as an oxidation product [39].

According to FTIRS and DEMS data, strongly adsorbed intermediates are oxidized to CO_2. In the presence of bulk AA the same intermediates can be involved in reactions producing CO_2. We have shown that at least four different processes must be considered.

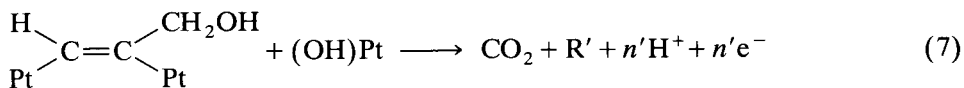(i) The oxidation of adsorbed CO (adsorbate C) takes place in the double layer and PtOH region:

$$(CO)Pt + (OH)Pt \longrightarrow CO_2 + H^+ + e^- + Pt \tag{6}$$
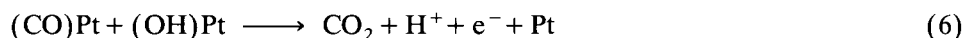
$$(C)$$

(ii) A second oxidation process involving an oxygen-containing adsorbate occurs in the same potential region:

$$\underset{Pt}{\overset{H}{\diagdown}}C=C\underset{Pt}{\overset{CH_2OH}{\diagup}} + (OH)Pt \longrightarrow CO_2 + R' + n'H^+ + n'e^- \tag{7}$$

(A)

Reactions (6) and (7) both give rise to the first peak of the voltammogram at ca. 0.90 V (Fig. 3).

(iii) Reactions producing the peak at ca. 1.10 V (Fig. 3) are predominant when AA is adsorbed at 0.25 V. The increase in the CH_3 band intensity and in the $CH_3:CH_2$ intensity ratio in the FTIR spectrum (Fig. 9) indicate that adsorbate B is likely to be oxidized under the second peak of the MSCV:

$$\underset{Pt}{\overset{H}{\diagdown}}C=C\underset{Pt}{\overset{CH_3}{\diagup}} + 6(O)Pt \longrightarrow 3CO_2 + 4H^+ + 4e^- + 8Pt \tag{8}$$
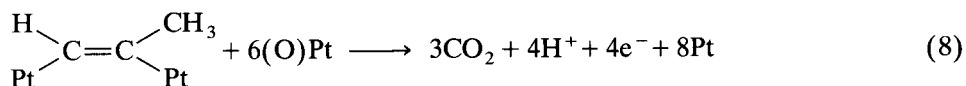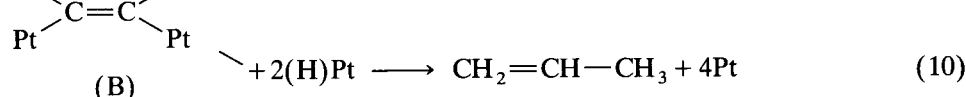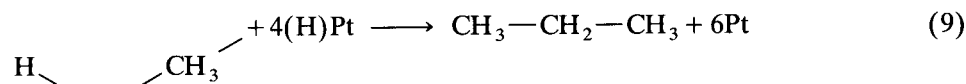
(B)

(iv) Parallel to reaction (8), oxidation of residues R (from reaction (3)) and R' (from reaction (7)) must occur.

Electroreduction reactions

At 0.05 V adsorbate B can be reduced to propane and propene through a hydrogenation reaction with PtH:

$$+4(H)Pt \longrightarrow CH_3-CH_2-CH_3 + 6Pt \tag{9}$$

$$\underset{Pt}{\overset{H}{\diagdown}}C=C\underset{Pt}{\overset{CH_3}{\diagup}}$$

(B)

$$+2(H)Pt \longrightarrow CH_2=CH-CH_3 + 4Pt \tag{10}$$

Ethane can be produced from the cleavage of adsorbate (D)

$$\underset{}{\overset{O}{\overset{\|}{}}}$$
$$H_2C=CH-C-Pt + 3(H)Pt \longrightarrow CH_3-CH_3 + (CO)Pt + 3Pt \tag{11}$$
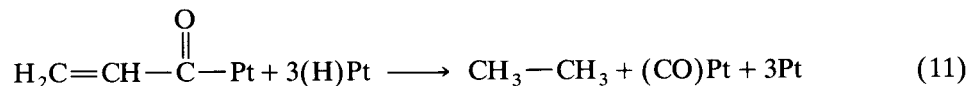
(D)

or from hydrogenation of the residue R formed in reaction (3).

Finally, propanol, which is observed only in the presence of bulk AA, is probably produced by reduction of the planar weakly adsorbed AA on Pt through hydrogenation of the double bond:

$$(CH_2=CH-CH_2OH)Pt_x + 2(H)Pt \longrightarrow CH_3-CH_2-CH_2OH + (x+2)Pt \tag{12}$$

General reaction scheme

All reactions are summarized in the following reaction scheme for AA on Pt in acids:

$$(AA)_{sol}$$

$$(CH_2=CH-C\overset{O}{\underset{}{\parallel}}H)_{sol} \xleftarrow{-H^+} (AA)Pt \xrightarrow{PtH} (n\text{-}PrOH)_{sol}$$
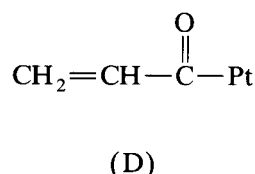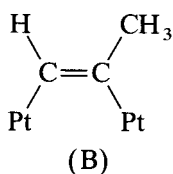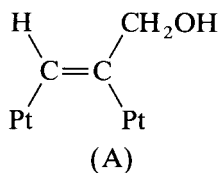

CONCLUSIONS

(i) Electroreduction of AA occurs in the Pt(H) potential region. These reactions imply the hydrogenation of the C=C bond, the C–OH splitting and the formation of adsorbed CO.

(ii) The electro-oxidation of bulk AA should involve weakly bound intermediates giving acrolein as the final product. The production of CO_2 is related to strongly bound adsorbates.

(iii) Strongly adsorbed species from AA containing two (C,H or C,O) or three (C,H,O) different atoms are detected, mostly keeping the C–C–C chain.

(iv) The DEMS and FTIRS data suggest that the following strongly bound adsorbates are formed:

$$\begin{array}{cccc}
\underset{Pt}{\overset{H}{\diagdown}}C=C\underset{Pt}{\overset{CH_2OH}{\diagup}} & \underset{Pt}{\overset{H}{\diagdown}}C=C\underset{Pt}{\overset{CH_3}{\diagup}} & \overset{O}{\underset{Pt}{\overset{\|\|}{C}}} & CH_2=CH-\overset{O}{\overset{\|}{C}}-Pt \\
(A) & (B) & (C) & (D)
\end{array}$$

The relative contribution of these species is $A \simeq B \gg C \simeq D$. Residues containing two C atoms and H must also be formed, but their structures could not be established.

ACKNOWLEDGEMENTS

REFERENCES

1 L.H. Little, N. Sheppard and D.J.C. Yates, Proc. R. Soc. London Ser. A, 259 (1960) 242.
2 M. Byrne and A.T. Kuhn, J. Chem. Soc. Faraday Trans. I, 68 (1972) 355.
3 M. Byrne and A.T. Kuhn, J. Chem. Soc. Faraday Trans. I, 68 (1972) 1898.
4 K. Fujikawa, H. Kita and K. Miyahara, J. Chem. Soc. Faraday Trans. I, 69 (1973) 481.
5 G. Semrau, Ph.D. Thesis, University of Bonn, 1984.
6 Yu.B. Vassiliev, V.S. Bagotzky, O.A. Khazova, V.V. Cherny and A.M. Meretsky, J. Electroanal. Chem., 98 (1979) 253.
7 I. Willner, M. Rosen and Y. Eichen, J. Electrochem. Soc., 138 (1991) 434.
8 Zh.I. Bobanova, G.A. Bodanovskii and G.D. Vovchenko, Electrokhimiya, 6 (1970) 909.
9 G. Horányi, G. Inzelt and K. Torkos, J. Electroanal. Chem., 101 (1979) 101.
10 G. Horányi and K. Torkos, J. Electroanal. Chem., 111 (1980) 279.
11 G. Horányi, Electrochim. Acta, 31 (1986) 1095.
12 J.Y. Gui, B.E. Kahn, C.H. Lin, F. Lu, G.N. Salaita, D.A. Stern, D.C. Zapien and A.T. Hubbard, J. Electroanal. Chem., 252 (1988) 169.
13 S.A. Chaffins, J.Y. Gui, C.H. Lin, F. Lu, G.N. Salaita, D.A. Stern, B.E. Kahn and A.T. Hubbard, J. Electroanal. Chem., 284 (1990) 67.
14 E. Pastor, M.C. Arévalo, S. González and A.J. Arvia, Electrochim. Acta, 36 (1991) 2003.
15 M.C. Arévalo, E. Pastor, S. González and A.J. Arvia, Electrochim. Acta, 36 (1991) 2183.
16 M.C. Arévalo, C. Gomis-Bas, E. Pastor, S. González and A.J. Arvia, Electrochim. Acta, 37 (1992) 1083.
17 R. Celdrán and J. González-Velasco, Electrochim. Acta, 26 (1981) 763.
18 E. Pastor, V.M. Schmidt, T. Iwasita, M.C. Arévalo, S. González and A.J. Arvia, Electrochim. Acta, in press.
19 L.B. Shapovalova and G.D. Zakumbaeva, Electrokhimiya, 13 (1977) 1331.
20 O. Wolter and J. Heitbaum, Ber. Bunsenges. Phys. Chem., 88 (1984) 2.
21 B. Bittins-Cattaneo, E. Cattaneo, P. Königshoven and W. Vielstich in A.J. Bard (Ed.), Electroanalytical Chemistry: A Series of Advances, Vol. 17, Dekker, New York, 1991, p. 181.

22 A. Bewick and S. Pons in R.J.H. Clark and R.E. Hester (Eds.), Advances in Infrared and Raman Spectroscopy, Vol. 12, Heyden, London, 1985, Ch. 1.

23 J.K. Foley and S. Pons, Anal. Chem., 57 (1985) 945.

24 E. Pastor, S. Wasmus, T. Iwasita, M.C. Arévalo, S. González and A.J. Arvia, J. Electroanal. Chem., 350 (1993) 97.

25 E. Stenhagen, S. Abrahamsson and F.W. McLafferty (Eds.), Atlas of Mass Spectral Data, Interscience, New York, 1969.

26 F.C. Nart and T. Iwasita, J. Electroanal. Chem., 308 (1991) 277.

27 A. Wieckowski, P. Zelenay and K. Varga, J. Chim., 88 (1991) 1247.

28 Standard Grating Spectra, Sadtler Research Laboratories Inc., Philadelphia, PA, 1973.

29 S.A. Francis, J. Chem. Phys., 18 (1950) 861.

30 G. Blyholder and L.D. Neff, J. Catal., 2 (1963) 138.

31 L.H. Little, Infrared Spectra of Adsorbed Species, Academic Press, London, 1966.

32 N. Sheppard and T.T. Nguyen in R.J.H. Clark and R.E. Hester (Eds.), Advances in Infrared and Raman Spectroscopy, Vol. 5, Heyden, London, 1978, p. 67.

33 T. Iwasita and F.C. Nart, J. Electroanal. Chem., 317 (1992) 291.

34 T. Iwasita, F.C. Nart, W. Vielstich and B. López, Electrochim. Acta, 37 (1992) 2361.

35 R.T. Morrison and R.N. Boyd, Química Orgánica, Fondo Educativo Interamericano, Bogotá, 1976, Chs. 15, 16, p. 507.

36 W.E. Triaca, T. Rabockai and A.J. Arvia, J. Electrochem. Soc., 126 (1979) 218.

37 W. Carruthers, Some Modern Methods of Organic Synthesis, Cambridge University Press, Cambridge, 1978.

38 B.B. Damaskin, O.A. Petrii and V.V. Batrakov, Adsorption of Organic Compounds on Electrodes, Plenum, New York, 1971, Ch. 8, p. 420.

39 M. Grayson and D. Eckroth (Eds.), Kirk-Othmer Encyclopedia of Chemical Technology, Vols. 1 and 2, Wiley–Interscience, New York, 1983.